Comparison of Control Strategies to Excite Intrinsic Oscillations in a SEA-Driven Robotic Joint

Annika Schmidt[1,2], Filip Pasic[1,3], Davide Calzolari[1,2], Arne Sachtler[1,2], Thomas Gumpert[2], Manuel Keppler[2] and Alin Albu-Schäffer[1,2]

***Abstract*— During the execution of periodic motions, such as locomotion, animals exploit the elasticity in their body to increase efficiency. Adding elasticity in robotic systems, e.g., through a Series Elastic Actuator (SEA), enables to mimic this biological solution by storing energy in the spring. The standard strategy to efficiently drive such systems in periodic motions is to assume the motor static such that the SEA behaves like a single-mass-spring system, excited at its natural frequency. However, when regarding the SEA as a two-mass-spring system, we can derive another control strategy to excite periodic oscillations, where the motor and link inertia exhibit anti-phasic oscillations. This paper compares these two control strategies on a hardware SEA test bed regarding performance metrics such as maximal input torque and electrical power consumption. The control objective for this comparison is to excite a link oscillation with a desired amplitude, as could be needed for a pick-and-place task. We find that less current is needed for the given task and hardware for the first control strategy. The second strategy causes more friction that needs compensation but also increases stored system energy for the desired amplitude. When adding motor inertia shaping to this second strategy, we find a flexible controller that can shift the system to either behave like a single- or two-mass-spring system. Thus, we propose a promising control approach that can adapt system behavior to best suit a given oscillatory task.**

I. Introduction

Inspired by the robustness and energy efficiency of biological systems, compliant elements are now often implemented in robotic systems [1], e.g., by adding a spring between the motor and link to create a Series Elastic Actuator (SEA). This makes systems more robust against external impacts and can aid in extending system run time when the elastic elements are efficiently exploited to store and release mechanical energy [2], [3]. However, adding elasticity to robotic systems also implies increased control complexity. The decoupling of a link and its actuator by means of a spring results in an underactuated system, where the elasticity can cause unwanted oscillations that need active vibration damping.

Traditionally, a passivity-based controller can establish desired impedance in a SEA system through indirect damping of the motor side [4]. However, this reduces the elasticity and thus negates the intended benefits of compliance. Expanding the control by a virtual motor coordinate through the Elastic Structure Preserving (ESP) controller [5], link side impedance can be restored in the underactuated system while still being able to make use of the compliance. Paired with established methods to compensate signal distortion through motor dynamics [6], [7], classic tracking tasks can then be realized with compliant robots with similar accuracy as seen for rigid solutions [8]. However, especially for highly dynamic motions like fast pick-and-place tasks, compliant robots bear the potential to outperform rigid systems due to the storing capacity of the elastic elements [9], [10]. Experiments showed that driving a compliant system with a human-inspired bang-bang controller [11] along its intrinsically preferred motions led to energy optimal trajectories [12]. Thus, to reap the benefits of compliance in terms of efficiency, it seems crucial that the controller is aware of the intrinsic dynamics of the system [13], [14]. Usually, only the link dynamics is considered, while the actuator is solely a means to generate force, and motor inertia effects need to be compensated. However, especially for heavy actuators, exploiting the motor inertia might bear the potential to increase energy efficiency in dynamic motions. This would lower power consumption and, thus, costs, e.g., for robots performing pick-and-place tasks in an industry setting.

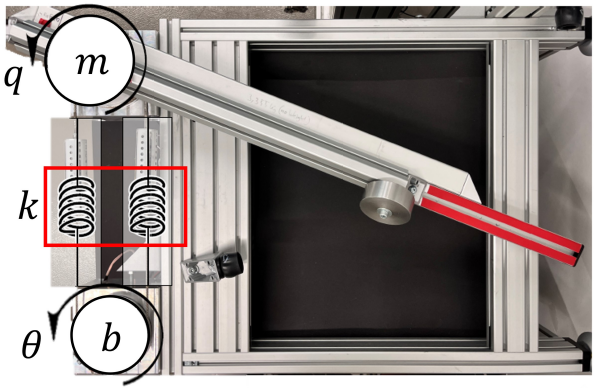

Fig. 1. Top view of the horizontally arranged system of one SEA-driven compliant joint, where the motor with inertia b drives a joint with inertia m coupled through a spring with stiffness k. The motor and joint coordinates are denoted θ and q, respectively.

Based on these hypotheses, this paper investigates two possible control strategies to excite intrinsic motions in a simple SEA-driven robotic joint usable for a basic pick-and-place task (Fig. 1). The first strategy controls the SEA to behave like a single mass-spring system, where only the link is excited. In contrast, the second strategy excites the SEA as a two-mass-spring system, where both the link and

This research was supported by the Advanced Grant M-Runners (Grant Agreement No. 835284) by the European Research Council (ERC).

[1] Technical University of Munich, TUM School of Computation, Information and Technology, Garching Germany an.schmidt@tum.de

[2]German Aerospace Center, Institute of Robotics and Mechatronics, Wessling, Germany

[3]Department of Electrical Engineering and Information Technology, University of Applied Sciences Munich, Germany

motor inertia oscillate against each other. This entails that depending on the applied controller, the SEA system will exhibit different natural frequencies. The linearity of the presently considered simple system allows us to calculate these frequencies analytically for verification, although we are aware that those do not exist in this way in nonlinear systems [15]. Thus, the presented control strategies do not rely on this prior system knowledge with the underlying hope of facilitating an extension of the controllers to more complex systems in the future. To compare the control strategies, the common control objective is defined to sustain a link oscillation with fixed amplitude to emulate the need of a pick-and-place task. The comparable metrics are the required maximal input torque and electrical power consumption as well as the stored system energy. To set the performance of the investigated controllers into perspective, the task is repeated with the ESP controller [5] as an established benchmark to drive compliant systems.

II. System and Setup

The proposed control concepts are initially validated on a compliant SEA-driven robotic joint (Fig. 1). The control signal u drives the motor inertia b connected to a link inertia m through a spring of stiffness k. The positions of the motor and link are denoted θ and q, respectively. The setup is arranged to swing horizontally neglecting gravitational influences. The system dynamics is

$$m\ddot{q} = k(\theta - q) \ , \tag{1}$$

$$b\ddot{\theta} + k(\theta - q) = u \ . \tag{2}$$

When controlling the system as a single-mass-spring system with a quasi-fixed motor the eigenfrequency f_{1m} of the link can be approximated by

$$2\pi \ f_{1m} = \sqrt{\frac{k}{m}} \ . \tag{3}$$

When the motor is substantially moving, the SEA system behaves like a two-mass-spring system with the combined mass $M = b + m$. The *reduced mass* μ of the coupled system [16] is defined by

$$\mu = \frac{mb}{b+m} = \frac{mb}{M} \ , \tag{4}$$

such that eigenfrequency of the oscillating masses will be

$$2\pi \ f_{2m} = \sqrt{\frac{k}{\mu}} \ . \tag{5}$$

In the considered hardware setup (Fig. 1), a single joint unit of the KUKA LWR 4 [17] is used as an actuator, which includes a Harmonic Drive. The arising friction caused by the actuator drive train is compensated through a well-tested friction observer [7]. All relevant parameters of the hardware setup are listed in Table I. With these values, the above-defined eigenfrequencies of the single- and the two-mass-spring system result in $f_{1m} = 3.02$ Hz and $f_{2m} = 4.95$ Hz, respectively.

TABLE I

System and control parameters of the hardware setup

system parameters			variables and metrics	
Link inertia	m	$1\,\mathrm{kg\,m^2}$	Electrical work	W_{el}
Motor inertia	b	$0.6\,\mathrm{kg\,m^2}$	Friction work	W_{fric}
Joint stiffness	k	$362\,\mathrm{N\,m\,rad^{-1}}$	Combined mass	M
1-mass frequency	f_{1m}	3.02 Hz	Reduced mass	μ
2-mass frequency	f_{2m}	4.95 Hz	Relative position	ϕ
Actuator limits		$\pm\ 100\,\mathrm{N\,m}$	COM position	ψ
Control rate		$3000\,\mathrm{Hz}$		

To quantitatively compare the different control approaches, parameters such as the maximum commanded torque $|u_{cmd}|$ and the required effort to compensate friction W_{fric} will be used as metrics. Additionally, the total system energy will be considered

$$E_{msr} = \frac{1}{2}b\dot{\theta}^2 + \frac{1}{2}k(\theta - q)^2 + \frac{1}{2}m\dot{q}^2 \ . \tag{6}$$

Furthermore, a current sensor (*EtherCAT EL3681, Beckhoff*) measures the mean current $i_{msr} > 0$ drawn from the power source during the motor control. This measurement is used to calculate the electrical work W_{el} of the $U = 48\,\mathrm{V}$ system per period length T:

$$W_{el} = \int_0^T U \ i_{msr} \ dt. \tag{7}$$

III. Control Approaches

To compare the investigated control strategies that should either excite the SEA as a single- or two-mass-spring system, the control objective is to sustain a link-side oscillation with a fixed amplitude. To reach this amplitude, the controllers need to continuously inject energy into the system until the desired amplitude is reached. At this point, the reached energy level needs to be maintained. To realize this concept, we regulate the energy level by introducing a variable damping term d_u for both control strategies. This term should scale the control input based on the required energy level E_{des} to reach the desired amplitude of the link oscillation

$$d_u = (E_{des} - E_{msr})\dot{q} \ . \tag{8}$$

The specific control laws to inject the excitation energy for each control strategy are detailed in the following.

A. Exciting link dynamics

We present two approaches to implement the first control strategy that should primarily excite the link dynamics with an oscillation frequency f_{1m}. The first approach, *1m-Track*, is a common tracking controller, while the second, *1m-ESP*, is a variation of the established ESP-controller from [5]. Both controllers are detailed in the following.

1) 1m-Track: To only excite the link dynamics, the motor side should behave as if fixed (Fig. 2a), such that the desired system behavior is

$$m\ddot{q} = k(q_d - q) + d_u \ , \tag{9}$$

with q_d being a constant equilibrium position of the link.

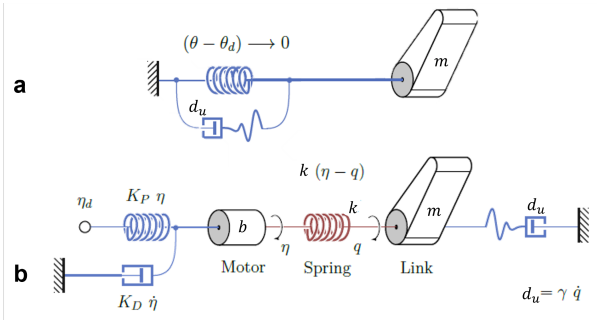

Fig. 2. Graphical representation of the desired closed-loop behavior to control a SEA as a single-mass-spring system, where only the link motion is excited and the motor behaves quasi-fixed by means of (a) tracking control and (b) an adapted ESP control approach [5].

Let $\theta_d = q_d + k^{-1} d_u$ be the desired motor position, then in the limit case of the motor position error $\tilde{\theta} = \theta - \theta_d$ approaching zero, the behavior of (1)-(2) matches the desired behavior. Implementing the PD-like controller

$$u = b\ddot{\theta}_d + k(\theta - q) - K_D\dot{\tilde{\theta}} - K_P\tilde{\theta}\ , \tag{10}$$

where K_P and K_D are positive proportional and derivative gains, respectively, results in a cascade closed loop, where $(\tilde{\theta}, \dot{\tilde{\theta}}) \to (0,0)$ for $t \to \infty$.

2) 1m-ESP: Originally, the ESP-controller [5] was designed to achieve motion tracking and inject link-side damping. In the here applied variation of this controller, the damping term regulates the energy level to achieve the desired oscillation amplitude of the link (Fig. 2b). Adding a new motor coordinate η yields the dynamics described by

$$m\ddot{q} = k(\eta - q) + d_u\ , \tag{11}$$

$$b\ddot{\eta} + k(\eta - q) + K_D\dot{\eta} + K_P(\eta - \eta_d) = 0\ , \tag{12}$$

where $K_D > 0$ and $K_P > 0$ determine the motor side impedance and $\eta_d = q_d$ defines the desired equilibrium link position. Comparing this desired link behavior in (11) with the dynamics of the real system (1) results in

$$\eta = \theta - k^{-1} d_u\ . \tag{13}$$

Setting the desired motor behavior from (12) in relation to the plant motor dynamics in (2) leads to the control command

$$u = k^{-1} b\ddot{d}_u + d_u - K_P(\eta - \eta_d) - K_D\dot{\eta}\ . \tag{14}$$

Since the controllers will only be compared for the steady state behavior, where the energy level is constant to reach the desired oscillation amplitude, all derivatives of d_u are zero.

B. Exploiting motor inertia

A novel idea investigated in this research is whether exploiting a system's motor inertia could entail an energetic benefit in a dynamic motion task. For this, the SEA chain should behave like a two-mass-spring system (Fig. 3a). When supporting this system's intrinsic dynamics through adding the damping term d_u from (8), an oscillation with the eigenfrequency of f_{2m} as in (5) should be excited. To apply the variable damping d_u to the two-mass spring system, it is transformed into a pair of decoupled one-body problems as proposed by [16]. The first problem characterizes the stiff properties of the system (Fig. 3b), while the second problem captures the elasticity of the system (Fig. 3c). As described in (4), the combined system has the reduced mass μ. According to [16], the elastic force of the two-mass system suggests the relative position as the first generalized coordinate

$$\phi = \theta - q\ . \tag{15}$$

The second generalized coordinate is the resulting position of the center of mass (COM)

$$\psi = \frac{b\theta + mq}{M}\ . \tag{16}$$

The system behaviors of the two replacement one-mass systems can then be described by the equations of motion

$$\mu\ddot{\phi} + k\phi = \frac{m}{M}u\ , \tag{17}$$

$$M\ddot{\psi} = u\ , \tag{18}$$

where the control signal u should excite the intrinsic oscillation of the combined system according to the damping term in (8). Since the motor should now move substantially, the system energy E_{msr} is expected to be higher, such that the defined energy level E_{des} to reach the desired link oscillation amplitude will differ with this control strategy from the energy needed by the strategies to excite the SEA as a single-mass spring system. The controller to excite the two-mass-spring system is denoted *2m-SC* in the following. For details and proof of the applied decoupling method, refer to [16].

One intriguing extension when applying a control scheme that uses the motor inertia is to investigate the influence of inertia shaping [4], [18] on the motor side. By adding a feedback loop from the estimated spring torque $\tau = k(\theta - q)$, the motor dynamics can be altered to behave as if the motor inertia was changed to β, i.e., increasing or decreasing the mass of this body in the two-mass-spring system. The motor inertia can be shaped from b to β by

$$u = b\beta^{-1}u' + (1 - b\beta^{-1})\tau\ , \tag{19}$$

where u' becomes the new input variable. For details on inertia shaping, refer to [4].

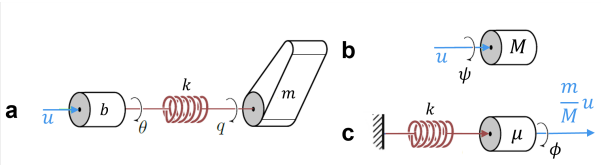

Fig. 3. (a) Initial SEA system that should be controlled to behave as a two-mass-spring system. Applying a coordinate transformation to divide the system into two one-body problems, where (b) one represents a system with rigid dynamics with the combined mass M moving along the position ψ and (c) a flexible problem with the reduced mass μ capturing the elasticity through the distance of the individual masses ϕ (adapted from [16]).

IV. Experimental Controller Comparison

To compare how the different control strategies excite a compliant robotic joint and investigate whether the motor mass exploitation bears a potential benefit, all controllers were implemented on the hardware system shown in Fig. 1. The choice to investigate the controllers directly in hardware (instead of conducting a simulation study first) was driven by the expectation that the performance of the controllers is heavily influenced by the motor dynamics and occurring friction. Accurately modeling these dynamics is challenging and usually requires extensive hardware characterization [19]. Thus, we focused on testing the approaches in hardware for the assessment of their applicability. The parameters of each controller were tuned such that they all excited a link oscillation of ± 0.05 rad amplitude. The averaged steady-state motions over 25 periods were compared, while the transient was disregarded. In addition to the derived approaches, *1m-Track*, *1m-ESP* and *2m-SC*, the established *ESP*-Controller from [5] was implemented to excite the oscillation as a baseline reference. This reference was applied with three different frequencies for the desired amplitude: first, a slow motion, where the link could follow the commanded motor position, and then the hardware frequencies of f_{1m} and f_{2m}, as a comparison to the investigated new control strategies.

A. Exciting fixed amplitude oscillations

As expected, the *1m-Track* and *1m-ESP* controllers designed to excite the SEA as a single-mass-spring system, commanded little motion to the motor while exciting comparatively large link oscillations. The tracking controller *1m-Track* led to an oscillation frequency that matched precisely the expected frequency of f_{1m} =3.0 Hz (Fig. 4a). With the *1m-ESP* controller, the motor moved slightly more, leading to a decreased frequency of 2.9 Hz (Fig. 4b). In contrast, the *2m-SC* excited the anti-phasic behavior of a two-mass-spring system as intended. Due to the inertia relation of 0.6 : 1, the

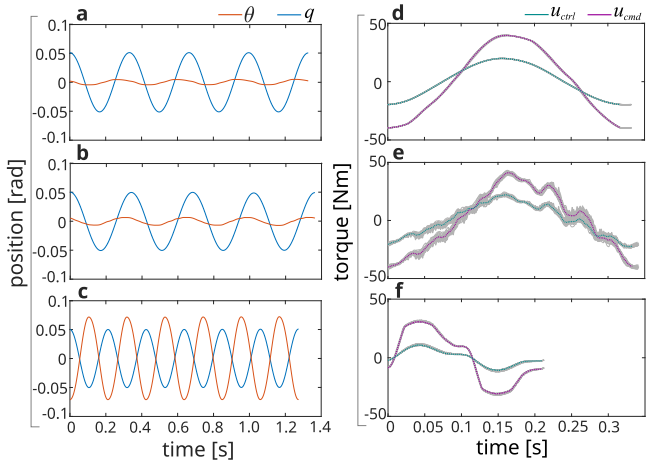

Fig. 4. System behavior as excited by the (a,d) *1m-Track*, (b,e) *1m-ESP* and (c,f) *2m-SC* controllers. (a-c) shows the position coordinates θ of the motor (orange) and q of the link (blue), while (d-f) shows the calculated control torques u_{ctrl} before friction compensation (cyan) and the eventually commanded torque u_{cmd} (magenta) after friction compensation. The shown torque values are depicted for one period averaged over 20 periods.

TABLE II

Summary of comparative controller metrics per period

Controller	f [Hz]	i_{msr} [mA]	u_{cmd} [N m]	W_{fric} [J]	W_{el} [J]	E_{msr} [J]
1m-Track	3.0	126	40.3	0.21	2.0	0.44
1m-ESP	2.9	128	41.4	0.36	2.1	0.38
2m-SC	4.7	533	33.5	5.19	5.45	2.58
ESP slow (ref.)	0.3	79	14.1	1.42	12.7	0.004
ESP f_{1m} *(ref.)*	3.0	122	37.6	0.21	2.0	0.42
ESP f_{2m} *(ref.)*	4.7	513	38.2	4.90	5.2	2.57

motor showed a higher oscillation amplitude than the link (Fig. 4c). The oscillation frequency of the coupled system was with 4.7 Hz slightly lower than determined for f_{2m}. However, a simulation of the frictionless system validated that the controller theoretically excites the correct frequency of 4.9 Hz. The decrease in the hardware setup is most likely caused by imperfections and friction losses that cannot be compensated. This validates that the applied control strategies indeed excite the intended system dynamics.

However, the more interesting question is whether any of the applied strategies have benefits over the other ones. It was expected that controlling a stiffer motor behavior would result in much higher commanded torques to hold the motor steady. In contrast, the torques of the oscillating two-mass-spring system should be noticeably lower with higher motor amplitude and velocity. As apparent from Fig. 4d-f (cyan), the calculated torque u_{ctrl} with the *2m-SC* controller is indeed only 65 % of the torque needed by the other two controllers. However, after the friction observer adds torque to account for the internally arising losses, in the eventually commanded torques u_{cmd} this difference reduces to 83 % (Fig. 4d-f, magenta). Comparatively, more friction must be compensated when the motor moves instead of behaving stiffly. This is also reflected in the work applied by the friction observer on the motor over one period τ_{fric} shown in Table II. As this metric includes the motor velocity, which is virtually zero when only the link dynamics are excited, the carried-out friction work is 15 times higher for the *2m-SC* control strategy. For all compared metrics, the values of the *1m-Track* and *1m-ESP* are of similar magnitude, with the latter performing slightly worse, most likely due to the noisier control signal caused by the feedback term included in the virtual motor coordinate η (Fig. 4e). Due to the increased motor motion and needed friction compensation of the two-mass-spring system, the mean drawn current i_{msr} is more than four times higher than when the motor behaves stiffly. Nevertheless, it must be noted that considerably more energy is stored in the two-mass-spring system as quantified by E_{msr} (Tab. II) since the additional motion of the motor leads to a much higher deflection of the spring.

When applying the hardware frequencies f_{1m} and f_{2m} with the established ESP approach [5], the same behaviors as with the respective control strategies to excite the SEA as single- or two-mass-spring system can be seen as reflected by the similarity of the metrics (Tab. II, *ESP 1m* and *2m*). When commanding the motor with a much lower frequency, such that the link can almost ideally follow, the drawn current

is overall lowest. Still, τ_{fric} indicates that the slow motion causes more friction than when the motor is held in position. The electrical work W_{el} is also considerably higher than with all other control strategies due to the long period time. Since the spring is not used at all to store energy in this slow motion, the system energy E_{msr} is lowest with this approach.

Summarizing these observations, for the given oscillation task with fixed amplitude, the control strategy that commands the SEA to behave like a single-mass-spring system, where only the link dynamics are excited, appears most beneficial regarding the required energy. When the SEA is controlled as a two-mass-spring system, the motor motion causes proportionally more friction that needs compensation, negating the anticipated benefit of exploiting the motor's inertia. Comparison with the established *ESP* baselines also indicates that it is secondary, which controller is applied to realize a desired behavior. All controllers to excite the link dynamics only led to metric values of similar magnitude. Likewise, the metrics obtained with the *2m-SC* and the reference *ESP* for f_{2m} matched well. However, to excite the intrinsic dynamics with the *ESP* controllers [5] required prior knowledge of the system's natural frequencies. In contrast, all newly proposed methods were designed to inject energy along the current link velocity, which organically results in the correct frequencies. Although it did not seem beneficial for the given task to exploit the motor dynamics, it needs to be acknowledged that exciting the SEA as a two-mass-spring system allowed to inject and keep more energy in the system. This could be a promising feature for different tasks than the analyzed one. Therefore, the potential of the *2m-SC* controller is further investigated in the following section.

B. Influence of motor inertia on two-mass oscillation

To get more insight into the potential of the *2m-SC* controller and the influence of the motor inertia on the system behavior, another hardware experiment was carried out. In the same setup (Fig. 1), the perceived inertia β of the motor side was changed through inertia shaping described in (19). Here, the oscillation amplitude of the link was not fixed, but instead, the system energy E_{msr} should be constant ($\approx 1.1\,\mathrm{J}$). However, it became apparent that for shaped inertias smaller than the physical motor one ($b = 0.6$), the energy had to be increased to a minimum of $1.4\,\mathrm{J}$ to overcome the system friction and realize any motion. Additionally, for shaped inertias noticeably larger than the link inertia, the motor is anticipated to become sluggish and behave increasingly similarly to the single-mass-spring system. To validate this assumption, for such a case with $\beta = 2$, instead of fixing the system energy, here again, the same amplitude as in the previous experiment ($q_{max} = 0.05$rad) should be reached.

The resulting behavior for the changing inertia values is depicted in Fig. 5 and summarized in Table III. The lowest inertia value that could be shaped for stable system behavior was for $\beta = 0.25$, but is not explicitly listed as the behavior, and all metric values were identical to the ones for $\beta = 0.5$. When keeping the energy constant, increasing the perceived inertia β leads to an increase of the link oscillation amplitude

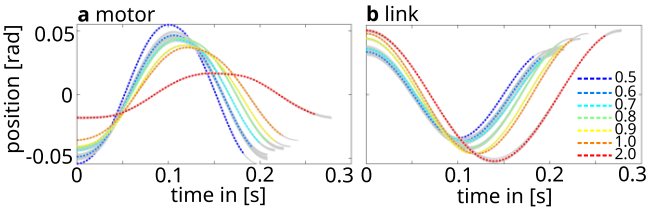

Fig. 5. Influence of shaped inertia of the motor β in $\mathrm{kg\,m^2}$ on the oscillation amplitude and frequency of the (a) motor coordinate θ, and the (b) link coordinate q plotted for the average of 20 oscillation periods.

(Tab. III, q_{max}), while at the same time, the motion amplitude of the motor decreases. Consequently, the needed work to compensate friction τ_{fric} and thus the electrical work W_{el} decrease with lower motor amplitudes. Shaping the motor inertia to match the link inertia results in an identical amplitude range for the motor and link side (Tab. III, $|q| - |\theta| \approx 0$). For the case of comparatively heavy motor inertia ($\beta = 2$), as expected, the motor moves much less than the link, indeed showing similar behavior to when the SEA was controlled to behave like a single-mass-spring system. As seen for the *1m-Track* and *1m-ESP* approaches, a higher torque u_{cmd} is applied to hold the motor while the work to compensate friction is considerably reduced. Likewise, the oscillation frequency of the system is with $3.6\,\mathrm{Hz}$ noticeably lower than the initial f_{2m} and closer to f_{1m}. Despite the higher link amplitude compared to $\beta = 1$, the system energy drops since the spring is less deflected with a stiffer motor. Increasing β even more in the hardware setup did not lead to a noticeably different behavior. Doing so in simulation to $\beta = 5$ excited an oscillation with $f = 3.3\,\mathrm{Hz}$. Doubling the inertia again only marginally reduced the oscillation frequency to $3.2\,\mathrm{Hz}$ by decreasing the motor motion slightly more. Thus, the inertia shaping appears to have the most noticeable effect for $b < \beta < 4b$, but it saturates for higher values and has limited applicability in hardware.

Summarizing the observations of the second experiment shows that the *2m-SC* control strategy paired with inertia shaping can excite different behaviors in the SEA system. When virtually decreasing the motor inertia, the dynamics of a two-mass-spring system are excited, which injects more energy into the system. Virtually increasing the motor inertia shifts the motor to behave progressively static, reducing the system energy and mainly exciting the link dynamics. This shift entails that different oscillation frequencies can be realized and that required torques and electrical consumption

TABLE III

METRICS COMPARING INERTIA SHAPING EFFECTS ON 2M-SC

β [$\mathrm{kg\,m^2}$]	E_{msr} [J]	f [Hz]	q_{max} [rad]	u_{cmd} [N m]	$\lvert q\rvert - \lvert\theta\rvert$ [rad]	τ_{fric} [W s]	W_{el} [W s]
0.5	1.4	5.0	±0.032	34.0	-0.023	3.2	3.7
0.6	1.1	4.8	±0.034	30.4	-0.016	2.9	3.4
0.7	1.1	4.6	±0.035	28.2	-0.010	2.6	3.2
0.8	1.1	4.4	±0.040	25.6	-0.003	2.5	3.1
0.9	1.1	4.3	±0.041	25.4	0.001	2.3	3.0
1.0	1.0	4.1	±0.044	27.6	0.007	2.1	2.9
2.0	0.7	3.6	±0.05	36.2	0.030	1.0	2.3

can be changed. Therefore, the *2m-SC* is a more flexible approach that can adapt the system behavior to suit different requirements. This control strategy could be helpful to maximize hardware capabilities, e.g., use a strong motor rather statically but exploit motor inertia when the torque is limited.

C. Limitations and future work

It must be acknowledged that the performance of the presented control strategies was only investigated for a single actuator type, i.e., an actuator with a harmonic drive. In a direct drive, lower frictional losses need less compensation, which should lower the overall torques and electrical power. This would especially benefit the *2m-SC* performance, which likely decreases the gap in electrical power consumption to the *1m*-controllers. Next to the actuator type, which controller is most beneficial also strongly depends on hardware properties, like motor-link inertia relation or used spring stiffness. Evaluating all these different aspects will be subject to future research, as the influences on the controller performance can be manifold. Although simulations with simplified models of different actuator types can provide first insights about how to best pair the control approaches, the presented experiment showcased the dominating influence of friction. Since this aspect is hard, if not impossible, to model accurately, validation in hardware will remain crucial. Additionally, the transient response and robustness against external disturbances should be investigated. However, good robustness can be expected since the controllers do not rely on precise model parameters but adapt to the intrinsic system oscillations. Furthermore, future work needs to expand the control theory to multi-joint and nonlinear systems.

V. Conclusion

We investigated two different control strategies to excite link oscillations of fixed amplitude in a compliant SEA-driven robotic joint with regard to required input torques and electrical power consumption. The first strategy controlled the SEA to behave like a single-mass-spring system with a quasi-fixed motor, while the second strategy also moved the motor inertia substantially, leading to a two-mass-spring system behavior. With the first control strategy, less electrical energy was consumed but higher torques were needed. Controlling the SEA to behave as a two-mass-spring system required lower torques, but this benefit was partly neglected since the increased motor motion caused more friction to compensate, resulting in higher electrical energy consumption overall. At the same time, however, moving the motor enabled to store more energy in the system. Adding inertia shaping to this approach showed the potential to design a flexible controller that can shift the behavior of the SEA system from the oscillation of a two-mass-spring system to a single-mass-spring system. Although more investigations are needed, these findings are encouraging, as they suggest the potential to view a motor not merely as an energy source but as a part of a complete system where all dynamic mechanical properties should be exploited through with more comprehensive approach.

Acknowledgments

The authors thank Robert Burger and David Wandinger for their support with the hardware test bed.

References

[1] R. Van Ham, T. G. Sugar, B. Vanderborght, K. W. Hollander, and D. Lefeber, "Compliant actuator designs," *IEEE Robotics & Automation Magazine*, vol. 16, no. 3, pp. 81–94, 2009.

[2] U. Scarfogliero, C. Stefanini, and P. Dario, "The use of compliant joints and elastic energy storage in bio-inspired legged robots," *Mechanism and Machine Theory*, vol. 44, no. 3, pp. 580–590, 2009.

[3] A. Velasco, M. Garabini, M. G. Catalano, and A. Bicchi, "Soft actuation in cyclic motions: Stiffness profile optimization for energy efficiency," in *International Conference on Humanoid Robots (Humanoids)*. IEEE, 2015, pp. 107–113.

[4] C. Ott, A. Albu-Schaffer, A. Kugi, and G. Hirzinger, "On the passivity-based impedance control of flexible joint robots," *IEEE Transactions on Robotics*, vol. 24, no. 2, pp. 416–429, 2008.

[5] M. Keppler, D. Lakatos, C. Ott, and A. Albu-Schäffer, "Elastic structure preserving (ESP) control for compliantly actuated robots," *IEEE Transactions on Robotics*, vol. 34, no. 2, pp. 317–335, 2018.

[6] H. Olsson, K. J. Åström, C. C. De Wit, M. Gäfvert, and P. Lischinsky, "Friction models and friction compensation," *Eur. J. Control*, vol. 4, no. 3, pp. 176–195, 1998.

[7] L. Le Tien, A. Albu-Schaffer, A. De Luca, and G. Hirzinger, "Friction observer and compensation for control of robots with joint torque measurement," in *International Conference on Intelligent Robots and Systems*. IEEE, 2008, pp. 3789–3795.

[8] M. Keppler, C. Raschel, D. Wandinger, A. Stemmer, and C. Ott, "Robust stabilization of elastic joint robots by ESP and PID control: theory and experiments," *IEEE Robotics and Automation Letters*, vol. 7, no. 3, pp. 8283–8290, 2022.

[9] B. Willems, J. Degrave, J. Dambre, *et al.*, "Quadruped robots benefit from compliant leg designs," in *International Conference on Intelligent Robots and Systems*. IEEE, 2017, pp. 3091–3091.

[10] C. Della Santina, C. Piazza, G. M. Gasparri, M. Bonilla, M. G. Catalano, G. Grioli, M. Garabini, and A. Bicchi, "The quest for natural machine motion: An open platform to fast-prototyping articulated soft robots," *IEEE Robotics & Automation Magazine*, vol. 24, no. 1, pp. 48–56, 2017.

[11] D. Lakatos, M. Görner, F. Petit, A. Dietrich, and A. Albu-Schäffer, "A modally adaptive control for multi-contact cyclic motions in compliantly actuated robotic systems," in *IEEE/RSJ Int. Conf. on Intelligent Robots and Systems*. IEEE, 2013, pp. 5388–5395.

[12] P. Stratmann, D. Lakatos, M. C. Özparpucu, and A. Albu-Schäffer, "Legged elastic multibody systems: adjusting limit cycles to close-to-optimal energy efficiency," *IEEE Robotics and Automation Letters*, vol. 2, no. 2, pp. 436–443, 2016.

[13] D. J. Braun, M. Howard, and S. Vijayakumar, "Exploiting variable stiffness in explosive movement tasks," *Robotics: Science and Systems VII*, vol. 7, pp. 25–32, 2012.

[14] A. Schmidt, B. Feldotto, T. Gumpert, D. Seidel, A. Albu-Schäffer, and P. Stratmann, "Adapting highly-dynamic compliant movements to changing environments: A benchmark comparison of reflex-vs. CPG-based control strategies," *Frontiers in Neurorobotics*, vol. 15, 2021.

[15] A. Albu-Schäffer and C. Della Santina, "A review on nonlinear modes in conservative mechanical systems," *Annual Reviews in Control*, vol. 50, pp. 49–71, 2020.

[16] M. Keppler and A. De Luca, "On time-optimal control of elastic joints under input constraints," in *2020 59th IEEE Conference on Decision and Control (CDC)*. IEEE, 2020, pp. 4149–4156.

[17] R. Bischoff, J. Kurth, G. Schreiber, R. Koeppe, A. Albu-Schäffer, A. Beyer, O. Eiberger, S. Haddadin, A. Stemmer, G. Grunwald, and G. Hirzinger, "The KUKA-DLR lightweight robot arm-a new reference platform for robotics research and manufacturing," in *International Symposium on Robotics*. VDE, 2010, pp. 1–8.

[18] A. Dietrich, X. Wu, K. Bussmann, M. Harder, M. Iskandar, J. Englsberger, C. Ott, and A. Albu-Schäffer, "Practical consequences of inertia shaping for interaction and tracking in robot control," *Control Engineering Practice*, vol. 114, p. 104875, 2021.

[19] S. Wolf and M. Iskandar, "Extending a dynamic friction model with nonlinear viscous and thermal dependency for a motor and harmonic drive gear," in *International Conference on Robotics and Automation*. IEEE, 2018, pp. 783–790.